Journal of Chemistry and Technologies, 2022, *30*(3), 378-385

Journal of Chemistry and Technologies

pISSN 2663-2934 (Print), ISSN 2663-2942 (Online).

journal homepage: http://chemistry.dnu.dp.ua

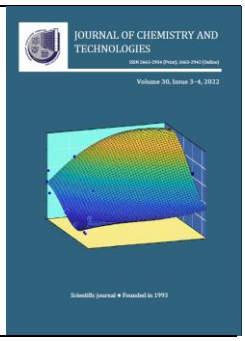

UDC 544.65+51-37

INFLUENCE OF UNSATURATED ORGANIC ACID ANIONS ON THE PROCESS OF ELECTROOXIDATION OF MANGANESE AQUACOMPLEXES (II)

Viktor F. Vargalyuk, Volodymyr A. Seredyuk, Kateryna A. Pliasovska, Igor M. Kuchai*

Oles Honchar Dnipro National University, 72, Gagarin Ave., Dnipro 49010, Ukraine

Received 25 August 2022; accepted 28 September 2022; available online 31 October 2022

Abstract

Using the methods of quantum-chemical modeling, the influence of unsaturated dibasic organic acids on the thermodynamic characteristics of the one-electron oxidation reaction of Mn^{2+} acidoacquacomplexes, which determine the basic level of energy efficiency of the electrochemical synthesis of MnO_2 , was investigated. It is shown that the monodentate anionic forms of maleic (HM^-) and fumaric (HF^-) acids do not have any advantages over the anions of monocarboxylic acids, in particular, acetate ions. On the contrary, the formation of hydrogen bonds with intraspherical water molecules by the second carboxyl group, which is not bound to the central atom, significantly impairs the effectiveness of the influence of HM^- and HF^- anions on the stage of electron extraction from the complexes $[Mn^{2+}(L)(H_2O)_5]$. The value of the standard redox potential E_0 (Mn^{2+}/Mn^{3+}) of ionic systems with single-charged anions of maleic and fumaric acids is 1.05 V and 0.99 V, respectively, which is much higher than E_0 (Mn^{2+}/Mn^{3+}) of acetate complexes (0.66 V), currently recommended for practical use. The presence in the internal coordination sphere of Mn^{2+} acid-acid complexes of bidentate-bonded double-charged maleic acid anion reduces E_0 (Mn^{2+}/Mn^{3+}) to 0.32 V, which is twice less than in acetate electrolyte. The prospects of maleate electrolytes are also enhanced by the ability of unsaturated anions M^{2-} to catalyze the disproportionation stage of Mn^{3+} complexes.

Keywords: complex compounds of manganese; fumaric and maleic acids; electrooxidation; DFT method.

ВПЛИВ АНІОНІВ НЕНАСИЧЕНИХ ОРГАНІЧНИХ КИСЛОТ НА ПРОЦЕС ЕЛЕКТРООКИСНЕННЯ АКВАКОМПЛЕКСІВ МАНГАНУ (II)

Віктор Ф. Варгалюк, Володимир А. Середюк, Катерина А. Плясовська, Ігор М. Кучай

Дніпровський національний університет імені Олеся Гончара, просп. Гагаріна, 72, Дніпро, 49010, Україна

Анотація

З використанням методів квантово-хімічного моделювання досліджено вплив ненасичених двоосновних органічних кислот на термодинамічні характеристики реакції одноелектронного окиснення ацидоаквакомплексів Mn^{2+}, які визначають базовий рівень енергоефективності процесу електрохімічного синтезу MnO_2. Показано, що монодентатні аніонні форми малеїнової (HM^-) та фумарової (HF^-) кислот не мають будь-яких переваг відносно аніонів монокарбонових кислот, зокрема, – ацетат-йонів. Навіть навпаки, утворення водневих зв'язків з внутрішньосферними молекулами води другою карбоксильною групою, яка не зв'язана з центральним атомом, суттєво погіршує ефективність впливу аніонів HM^- і HF^- на стадію вилучення електрона з комплексів $[Mn^{2+}(L)(H_2O)_5]$. Величина стандартного редокс-потенціалу $E_0(Mn^{2+}/Mn^{3+})$ йонних систем з однозарядними аніонами малеїнової і фумарової кислот становить 1.05 В і 0.99 В відповідно, що значно перевищує $E_0(Mn^{2+}/Mn^{3+})$ ацетатних комплексів (0.66 В), наразі рекомендованих до практичного використання. Присутність у внутрішній координаційній сфері ацидоаквакомплексів Mn^{2+} бідентатно зв'язаного двозарядного аніона малеїнової кислоти зменшує $E_0(Mn^{2+}/Mn^{3+})$ до 0.32 В, а це вдвічі менше, ніж в ацетатному електроліті. Перспективність малеїнатних електролітів посилюється також здатністю ненасичених аніонів M^{2-} каталізувати стадію диспропорціонування комплексів Mn^{3+}.

Ключові слова: комплексні сполуки Мангану; фумарова та малеїнова кислоти; електроокиснення; DFT-метод.

**Corresponding author: e-mail address: kuchay_i_n@ukr.net*

doi: 10.15421/jchemtech.v30i3.265467

Introduction

Synthetic manganese (IV) oxide is used in various fields [1–9]. Thus, MnO_2 nanoparticles are widely used in energy storage devices taking into account the vector of "green" energy [30], catalysts [30; 32; 33], sensors [23–26], adsorbents, biochemical and medical fields [34; 36]. The specific capacitance of such capacitors can reach 272 F/g (for the crystallographic form of δ-MnO_2) and 311 F/g (for γ-MnO_2), moreover, nanosheets retain up to 91 % of the initial capacity after 10,000 charge/discharge cycles. Crystalline phases have an advantage over amorphous phases, and the capacity increases in KI, Na_2SO_4 electrolytes, and more in the first one [27; 38]. In the electrocatalytic sense, the crystallographic form of α-MnO_2 nanoparticles has relatively high reducing properties with respect to O_2 and a powerful O_2-absorbing capacity [27]. A nanocomposite material consisting of a glassy carbon electrode modified with reduced graphene oxide (rGO) and incorporating MnO_2 nanowires has been shown to be promising for the sensitive and selective determination of bisphenol A (BPA) in plastic samples of household, food and medical use in the context of trace amount monitoring with a detection limit of 6.0 nmol/L [25]. Nanodispersed MnO_2 exhibits a promising bio-directed electrocatalytic property for the oxidation-reduction of H_2O_2, which has applications in the field of biomedicine, in particular in non-enzymatic biosensors of H_2O_2, thiols, glutathione, xenoestrogens. A new cellular 3D-electrochemical bioelectrosensor based on the identification of exocellular level of H_2O_2 (sensitivity was 0.02 μmol/L) by catalytic reaction with MnO_2 was developed for the *in vitro* evaluation of antioxidant activity of 16 anthocyanins and their glycoside derivatives as components of natural foods [23]. The technique is also used for the detection of NO_2^--ions taking into account pH and doped impurity ions that do not interfere with the identification of the former. The research of the authors [35] showed that nanodispersed MnO_2 and its composites can be used as antibacterial (against G+ and G– bacteria) and antifungal drugs, and the MnO_2/black cumin composite has prospects as an antibacterial agent for drinking water purification. Nanocomposite copolymer-MnO_2 is an effective material for wastewater treatment from organic pollutants [39]. Nanodispersed MnO_2 can potentially be used in MR imaging as well as targeted drug delivery. The high reactivity of highly dispersed MnO_2 with H_2O_2 cells can be used to alleviate cellular hypoxia in the treatment of some cancers. The catalytic tubular micrometer based on MnO_2 nanoparticles prepared by template electrodeposition can function as self-propelled therapeutic devices for anticancer drug delivery [27].

Electrochemical extraction of synthetic manganese (IV) oxide is traditionally carried out in sulfate electrolytes [10]. Their main drawback is that due to the high redox potential of the initial stage of the reaction

$Mn^{2+} - 2e^- + 2H_2O = MnO_2 + 4H^+$,

namely $Mn^{2+} - e^- = Mn^{3+}$ (E_0 = 1.51 V),

formation of the target product is accompanied by electro-oxidation of water (E_0 = 1.23 V):

$H_2O - e^- = \cdot OH + H^+$;

$2\cdot OH = H_2O + ½O_2$.

In addition to unproductive energy consumption, this leads to deterioration of the quality of the oxide film due to the loosening effect of gaseous oxygen.

In [11], the authors proposed to implement the electrooxidation of Mn^{2+} ions in acetate medium. As it turned out [12; 13], due to the entry of acetate ions into the internal coordination sphere of manganese aquacomplexes, the standard potential of the reaction $Mn^{2+} - e^- = Mn^{3+}$ decreases to 0.66 V, which is approximately 0.5 V more negative than the E_0 of the oxygen extraction process. However, since E_0 of the process of the next electron extractionfrom the intermediate $Mn(Ac)^{2+}$ remains very high (2.13 B [13]), and the elimination of the reaction $H_2O - e^- = \cdot OH + H^+$ removed the effective oxidant (OH-radicals) from the electrode surface, the formation of MnO_2 in acetate solutions occurs due to the disproportionation of $Mn(Ac)^{2+}$ complexes and the hydrolysis of the highly oxidized form of $Mn(Ac)^{3+}$. Trivalent manganese complexes $Mn(Ac)^{2+}$ are also prone to hydrolysis, therefore, the precipitate electrolytically released on the anode contains not only MnO_2 crystals, but also MnO(OH) [14; 15]. The ratio of these forms determines the catalytic properties of MnO_2 films, their adsorption activity, electrical conductivity and other physical and chemical characteristics.

Based on the above mechanism of the reaction of electrooxidation of $Mc(Ac)^+$ ions it is obvious that one of the most important factors influencing the composition of MnO_2 and the process of its production is the nature of the organic ligand, which should provide, on the one hand, a low oxidation potential of Mn^{2+} ions, and

on the other hand, a high rate of disproportionation of Mn^{3+} ions.

In order to improve the characteristics of the main stages of the electrochemical synthesis of MnO_2 , we considered it expedient to switch from monodentate ligands, which are acetate ions, to bidentate ones. Maleic and fumaric acids were chosen as the latter. Anions of these unsaturated acids in the composition of binuclear complexes Mn-L-Mn are able to act as an electron bridge in intramolecular redox processes.

Details of the initial stages of the reaction $Mn^{2+} - 2e^- = MnO_2$ in the presence of organic acid anions were investigated by quantum chemical modeling.

Research results and their discussion

Quantum chemical modeling was carried out using the Gaussian 09 program [16] and the Wachters+f basis set for manganese atoms and 6-311G for carbon, oxygen and hydrogen atoms [17]. The DFT method with B3LYP functional was used in the calculations [18; 19]. The solvent was taken into account using the polarization continuum DSM model [20; 21]. Other details are given in [13].

Table 1 presents the results of the calculations of the electron density distribution in the complexes $[Mn^{+z}(L)(H_2O)_n]$, and Fig. 1 shows their spatial structure. The octahedral structure, which is energetically the most advantageous for manganese aqua complexes, was taken as the basic model [13]. During the optimization process, it remained unchanged for all complexes, except for the compounds of manganese ions with M^{2-} , where the bidentate binding of fully deprotonated anions to the manganese cation leads to a natural decrease in the number of coordinated water molecules from 5 to 4 (z = 3), and to 3 (z = 2).

Table 1

Charge distribution on manganese atoms and ligands in $[Mn(L)(H_2O)n]^{z+}$ complexes

Complex	Central atom charge, e	Organic ligand charge, e	Total charge of water molecules, e
$Mn^{2+}(HM^-)(H_2O)_5$	1.1300	−0.6278	0.4948
$Mn^{3+}(HM^-)(H_2O)_5$	1.4260	−0.3125	0.8865
$Mn^{2+}(M^{2-})(H_2O)_3$	1.1140	−1.4660	0.3520
$Mn^{3+}(M^{2-})(H_2O)_4$	1.3496	−1.0081	0.6585
$Mn^{2+}(HF^-)(H_2O)_5$	1.1639	−0.6690	0.5051
$Mn^{3+}(HF^-)(H_2O)_5$	1.4599	−0.3883	0.9284
$Mn^{2+}(F^{2-})(H_2O)_5$	1.1510	−1.6240	0.4750
$Mn^{3+}(F^{2-})(H_2O)_5$	1.1590	−0.6780	0.5190

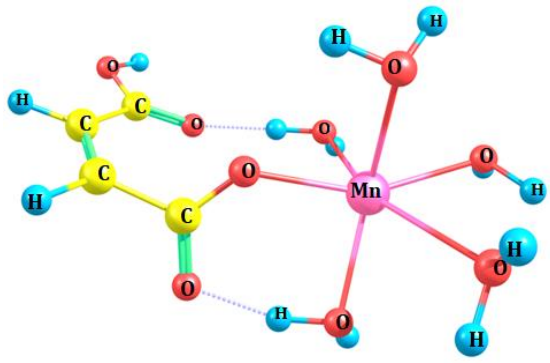

a)

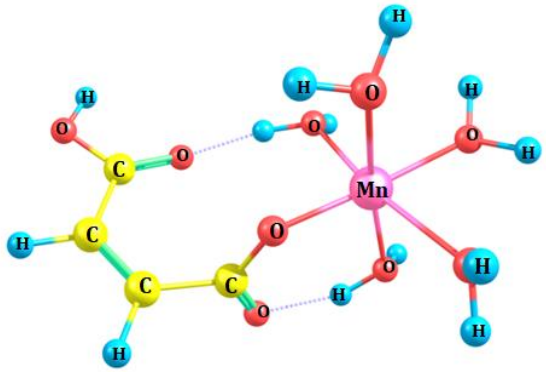

b)

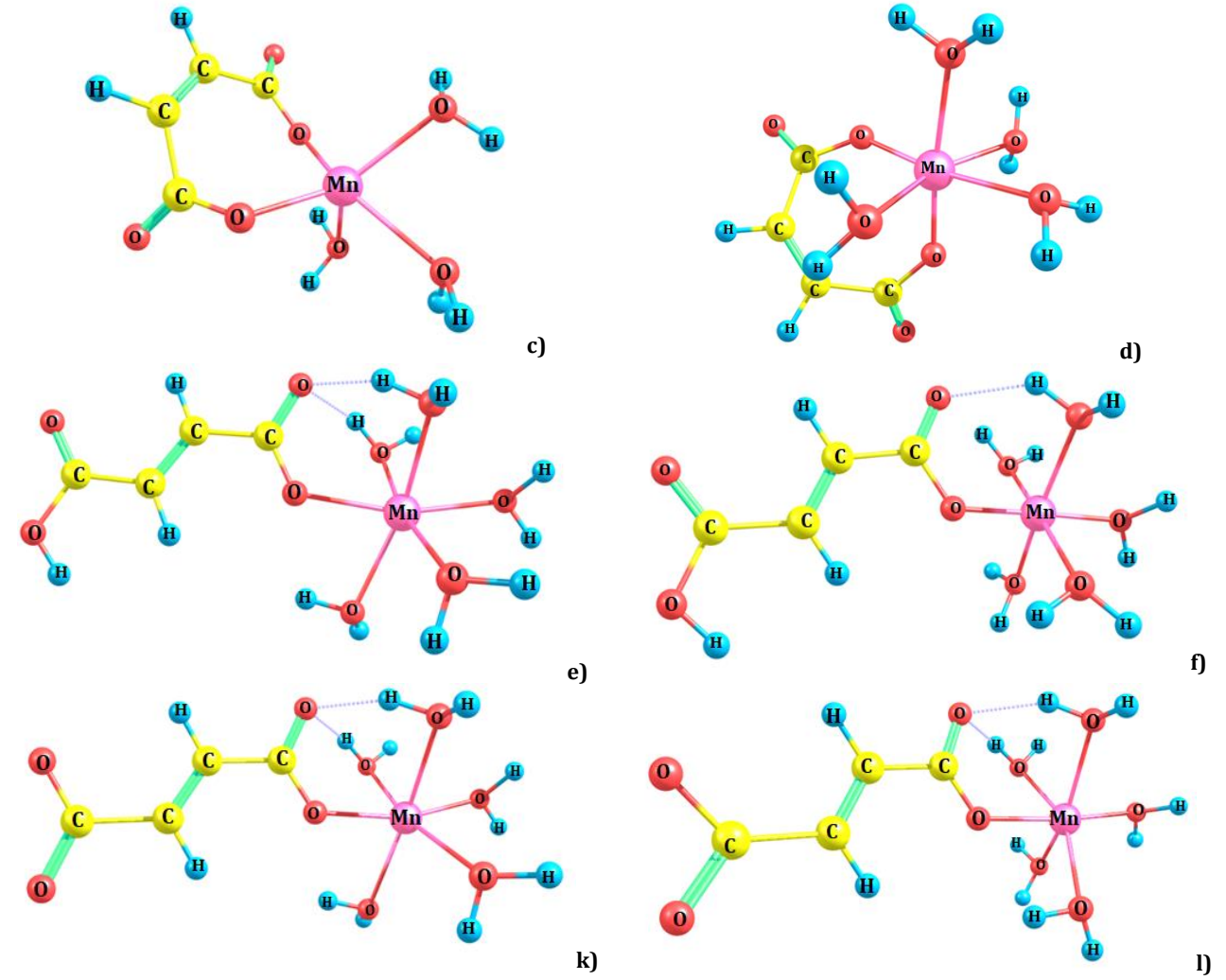

Fig. 1. Spatial structure of complexes a) $Mn^{2+}(HM^{-})(H_2O)_5$; b) $Mn^{3+}(HM^{-})(H_2O)_5$; c) $Mn^{2+}(M^{2-})(H_2O)_3$; (d) $Mn^{3+}(M^{2-})(H_2O)_4$; (e) $Mn^{2+}(HF^{-})(H_2O)_5$; (f) $Mn^{3+}(HF^{-})(H_2O)_5$; (k) $Mn^{2+}(F^{2-})(H_2O)_5$; (l) $Mn^{3+}(F^{2-})(H_2O)_5$

The complexes $[Mn^{3+}(M^{2-})(H_2O)_4]$ and $[Mn^{2+}(M^{2-})(H_2O)_3]$ are also characterized by the fact that the organic ligand does not form hydrogen bonds with intraspherical water molecules (Fig. 1c, d). In contrast, monoprotonated maleinate and fumarate ions are subject to such interaction (Fig. 1a, b, e, f). Hydrogen bonds are also formed by monodentate fumaric acid anions F^{2-} (Fig. 1k, l).

In [13], it was shown that when an electron is removed from homogeneous Mn^{2+} aquacomplexes, the charge of the central atom increases by 0.446 e, and 0.554 e is distributed approximately evenly between the six water molecules of the inner coordination sphere. It can be seen from Table 2 that in monosubstituted manganese acidoacqua complexes the degree of increase of the charge of the central atom becomes smaller, apparently, due to the greater electron donation of the anions of dibasic organic acids compared to the molecules of H_2O. Thus, in the case of single-charged ligands HM^{-} and HF^{-} Δ(Mn) it is 0.293e and 0.296e, respectively. When moving to the two-charged anions M^{2-} and F^{2-} the picture becomes different. In complexes with M^{2-}, the value of Δq(Mn) is close to the previous structures (0.2846e), while in complexes with F^{2-} the charge of the central atom almost does not change: Δq(Mn) = 0.018e. Consideration of the distribution of electron density between all structural elements showed that this was due to the fact that the electron was removed not from the orbitals of the manganese cation, but from the anion F^{2-} : $\Delta q(F^{2-})$ = 0.941e.

As can be seen from Table 2, with the unchanged value of Δq(Mn) in complexes with monoprotonated form of acid residues, the share of positive charge, which is localized on water molecules, is greater in the case of fumarate ions (0.4233e). Here $\Delta q(H_2O)$ exceeds even the corresponding value in maleate complexes with double-charged anion, in which $\Delta q(H_2O)$ = 0.3435e.

Table 2

Change of charge of structural elements of complexes $[Mn^{2+}(L)(H_2O)_n]$ at their one-electron oxidation

L	Δq(Mn)	Δq(L)	Δq(H_2O)
HM^-	0.2930	0.3153	0.3917
HF^-	0.2960	0.2807	0.4233
M^{2-}	0.2846	0.3719	0.3435
F^{2-}	0.0180	0.9410	0.0410

The revealed effect is explained by the geometric features of the structure of maleic and fumaric acids. As can be seen from Fig. 1a, b, the spatial arrangement of carboxyl groups in the HM^- anion allows both oxygen atoms of both -C=O fragments to form hydrogen bonds with hydrogen atoms of intraspherical water molecules. In complexes with HF^- only one –C=O fragment is available for such interaction (Fig. 1e, f).

Using the information about the change in the electronic energy of the clusters $[Mn^{2+}(L)(H_2O)_n](H_2O)_{5-n}$ at the removal of an electron from them $\Delta E_e = E_e\cdot\{Mn^{3+}(L)(H_2O)_x\} - E_e\cdot\{Mn^{2+}(L)(H_2O)_x\}$, we calculated the values of the standard potentials of the corresponding redox processes. They are given in Table 3.

The calculation was performed using the correlation formula $E_0 = -4.082 + 0.009\,\Delta E_e$ [22].

Table 3

Electronic energy values of manganese complexes, energetics and standard redox potentials of one-electron oxidation of Mn^{2+}

Complex	Electronic energy, Hartree E_e	Energy difference Mn^{2+}/Mn^{3+}, Hartree ΔE_e	Energy difference Mn^{2+}/Mn^{3+}, kJ/mol	E_0 (Mn^{2+} / Mn^{3+}), B
$Mn^{3+}(HM^-)(H_2O)_5$	–1987.98997	0.2170	570	1.05
$Mn^{2+}(HM^-)(H_2O)_5$	–1988.20127			
$[Mn^{3+}(M^{2-})(H_2O)_4](H_2O)$	–1987.54354	0.1864	489	0.32
$[Mn^{2+}(M^{2-})(H_2O)_3](H_2O)_2$	–1987.69875			
$[Mn^{3+}(HF^-)(H_2O)_5]$	–1987.97955	0.2148	564	0.99
$[Mn^{2+}(HF^-)(H_2O)_5]$	–1988.19392			
$[Mn^{3+}(F^{2-})(H_2O)_5]$	–1987.52635	0.1956	514	0.54
$[Mn^{2+}(F^{2-})(H_2O)_5]$	–1987.72198			

As expected, the bidentate binding of maleic acid anions significantly affected the energy of the process $Mn^{2+} - e^- = Mn^{3+}$ and, thus, the value of the standard potential. Its value dropped to 0.32 V, which is almost twice less relative to acetate complexes (E_0 = 0.66 V [13]).

It is characteristic that monodentate bound anions of dibasic acids affect E_0 to a lesser extent compared not only with bidentate M^{2-}, but also with acetate ions. Probably, the formation of the second carboxyl group of ions HM^-, HF^-, F^{2-} of a number of hydrogen bonds with intraspherical water molecules weakens their donor activity. In the absence of these bonds in both participants of the redox process $[Mn^{2+}(M^{2-})(H_2O)_3] - e^- = [Mn^{3+}(M^{2-})(H_2O)_4]$ the greatest decrease in E_0 is observed.

Taking into account the best indicators of the action of M^{2-} anions on the thermodynamic characteristics of the process $Mn^{2+} - e^- = Mn^{3+}$, we considered the second, no less important stage of the synthesis of MnO_2 – disproportionation of Mn^{3+} complexes, with their participation. For this purpose, a dimer of two complexes $[Mn^{3+}(M^{2-})(H_2O)_4]$ was created. After optimization, it took the form shown in Fig. 2a. The obtained binuclear structure $[(H_2O)_3Mn^{3+}(M^{2-})Mn^{3+}(M^{2-})(H_2O)_5]$ is definitely asymmetric due to the different composition of the nearest environment of Mn^{3+} ions. This naturally could not but affect the distribution of electron density in the dimer. Indeed, the charge of the manganese cation, with which both M^{2-} anions are in contact, is 1.4263e, while the second one is only 1.0903 e. The comparison of the obtained values with the values of charges of manganese cations in the complexes $[Mn^{3+}(M^{2-})(H_2O)_4]$ (1.3496) and $[Mn^{2+}(M^{2-})(H_2O)_3]$ (1.1140) in the first approximation indicates the realization of the disproportionation act in the presented binuclear system.

Journal of Chemistry and Technologies, 2022, *30*(3), 378-385

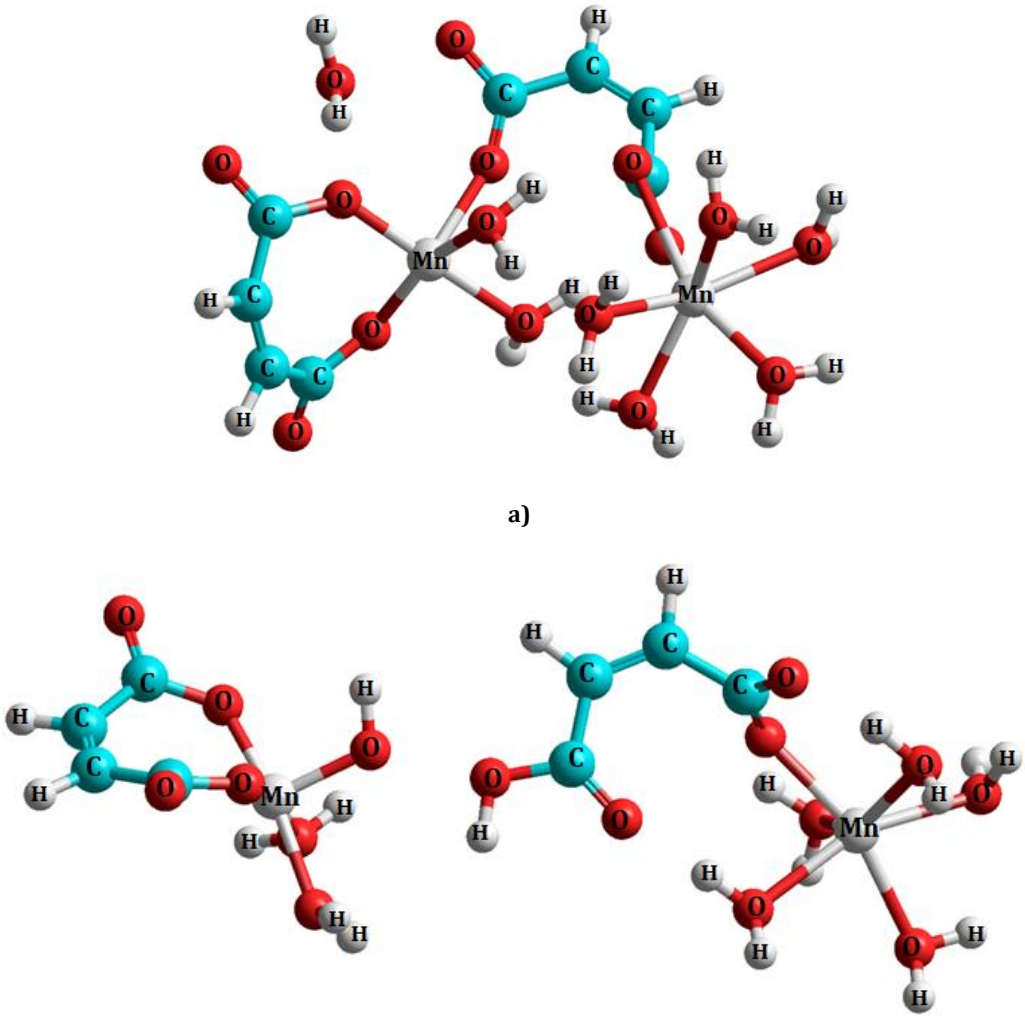

Fig. 2. Spatial structure of complexes a) Mn^{3+} (M^{2-})(H_2O)$_5$ Mn^{3+} (M^{2-})(H_2O)$_3$; (b) [Mn^{4+}(M^{2-})(OH^-)(H_2O)$_2$] and [Mn^{2+} (HM^-)(H_2O)$_5$]

The launch of fluctuation processes in the structure of the dimer revealed the possibility of migration of one of the protons of the water molecule, which is a ligand near the first manganese cation, to the carbon group of the anion M^{2-} , followed by the decomposition of the system into two stable particles [Mn^{4+}(M^{2-})(OH^-)(H_2O)$_2$] and [Mn^{2+}(HM^-)(H_2O)$_5$] (Fig. 2b). The found spin values of manganese cations in these complexes are 3.0332 and 4.8578, or rounded 3 and 5, respectively. In contrast to the charge values of the structural units of the molecular system according to Maliken, which differ significantly from the oxidation degrees, the spin values unambiguously indicate the type of ionic state of a particular atom. This allows us to affirmatively indicate the oxidation degrees of manganese in the formed complexes.

Since the energy of the formed complexes was 14 kJ/mol higher than the energy of the dimer, we can say that the disproportionation process of the complexes [Mn^{3+}(M^{2-})(H_2O)$_4$] has a small activation barrier.

Conclusions

Quantum-chemical study of the influence of dibasic organic acids on the thermodynamic characteristics of the one-electron oxidation of Mn^{2+} acido-aqua complexes has shown that in the case of monodentate binding of their anions, the system has no advantages over the anions of monocarboxylic acids, in particular, acetate ions. The formation of hydrogen bonds with intraspherical water molecules by the second carboxyl group, which is not bound to the central atom, significantly impairs the effectiveness of the monodentate forms on the stage of electron extraction from the complexes [Mn^{2+} (L)(H_2O)$_5$].

Thus, the value of E_0 (Mn^{2+} /Mn^{3+}) of ionic systems with single-charged anions of maleic and fumaric acids is 1.05 V and 0.99 V, respectively, which is much higher than E_0 (Mn^{2+} /Mn^{3+}) of

acetate complexes (0.66 V), currently recommended for practical use.

The presence of a bidentate double-charged maleic acid anion in the internal coordination sphere reduces E_0 (Mn^{2+} /Mn^{3+}) to 0.32 V, which is half that in acetate electrolyte.

The prospect of the use of maleic acid in the electrochemical synthesis of MnO_2 is further supported by the ability of M^{2-} anions to catalytically influence the disproportionation stage of the complexes $[Mn^{3+}(M^{2-})(H_2O)_4]$.

References

[1] Li, L., Scott, K., Yu, E. H. (2013). A direct glucose alkaline fuel cell using MnO_2 carbon nanocomposite supported gold catalyst for anode glucose oxidation. *Journal of Power Sources*, 221, 1–5. https://doi.org/10.1016/j.jpowsour.2012.08.021

[2] Moulav, M. H., Kale, B. B., Bankar, D., Amalnerkar, D. P., Vinu, A., Kanade, K. G. (2018). Green synthetic methodology: An evaluative study for impact of surface basicity of MnO_2 doped MgO nanocomposites in Wittig reaction. *Journal of Solid State Chemistry*, 269, 167–174. https://doi.org/10.1016/j.jssc.2018.09.028

[3] Tian, H., He, J., Liu, L., Wang, D., Hao, Z., Ma, C. (2012). Highly active manganese oxide catalysts for low-temperature oxidation of formaldehyde. *Microporous and Mesoporous Materials,* 151, 397–402. https://doi.org/10.1016/j.micromeso.2011.10.003

[4] Wu, J., Yuan, H., Zhang, P., Zhang, H., Wu, Y. (2016). Synthesis of glucuronic acid by heterogeneous selective oxidation with active MnO_2 characterized generally. *Reaction Kinetics, Mechanisms and Catalysis*, 117, 319–328. doi: 10.1007/s11144-015-0930-4

[5] Ye, D., Li, H., Liang, G., Luo, J., Zhang, X., Zhang, S., Chen, H., Kong, J. (2013). A three-dimensional hybrid of MnO_2 /graphene/carbon nanotubes based sensor for determination of hydrogen-peroxide in milk. *Electrochimica Acta,* 109, 195-200. http://dx.doi.org/10.1016/j.electacta.2013.06.119

[6] Wang, P., Sun, S., Wang, S., Zhang, Y., Zhang, G., Li, Y., Li, S., Zhou, C., Fang, S. (2017). Ultrastable MnO_2 nanoparticle/three-dimensional N-doped reduced graphene oxide composite as electrode material for supercapacitor. *Journal of Applied Electrochemistry, 47*(12), 1293–1303. https://link.springer.com/article/10.1007/s10800-017-1122-x

[7] Prasad, K. R., Miura N. (2004). Polyaniline-MnO_2 composite electrode for high energy density electrochemical capacitor. *Electrochemical and Solid-State Letters*, *7*(11), A425–A428. https://doi.org/10.1149/1.1805504

[8] Wei, W., Cui, X., Chen, W., Ivey D. G. (2011). Manganese oxide-based materials as electrochemical supercapacitor electrodes. *Chemical Society Reviews*, *40*(3), 1697–1721. https://doi.org/10.1039/c0cs00127a

[9] Yadav, G. G., Wei, X., Gallaway, J. W., Chaudhry, Z., Shin, A., Huang, J., Yakobov, R., Nyce, M., Vanderklaauw, N., Banerjee, S. (2017). Rapid electrochemical synthesis of δ-MnO_2 from γ-MnO_2 and unleashing its performance as an energy dense electrode. *Materials Today Energy,* 6, 198–210. https://doi.org/10.1016/j.mtener.2017.10.008

[10] Yakymenko, L. M. (1977). [Electrode materials in applied electrochemistry]. *Moscow: Chimiya*. (in Russian).

[11] Rusi, Majid S.R. (2014). Controlled synthesis of flower-like α-MnO_2 as electrode for pseudocapacitor application. *Solid State Ionics*, 262, 220–225. https://doi.org/10.1016/j.ssi.2013.10.003

[12] Poltavets, V. V. , Vargalyuk, V. F., Shevchenko, L. V. (2015). The peculiarities of electrooxidation of Mn^{2+} to MnO_2 in acetate electrolyte. *Bulletin of Dnipropetrovsk University. Series Chemistry, 23*(2), 27–31. https://doi.org/10.15421/081515

[13] Poltavets, V. V., Vargalyuk, V. F., Seredyuk, V. A., Shevchenko, L. V. (2018). The Mechanism of Electrooxidation of Mn^{2+} ions. *Journal of Chemistry and Technologies*, *26*(2), 1–11. https://doi.org/10.15421/0817260201

[14] Poltavets, V. V., Vargalyuk, V. F., Shevchenko, L. V. (2018). Express-method for Estimation of Electrocatalytic Activity of Oxide Films toward Oxygen Transfer Reactions. *Universal Journal of Chemistry, 6*(2), 15–20. doi: 10.13189/ujc.2018.060201

[15] Poltavets, V. V. , Hruzdieva, E. V. (2011). [Manganese dioxide as an electrode material]. *Bulletin of Dnipropetrovsk University. Series Chemistry, 19*(17), 34–38. (in Russian). https://www.dnu.dp.ua/visnik/fhim/6

[16] Frisch, M. J., Trucks, G. W., Schlegel, H. B., Scuseria, G. E., Robb, M. A., Cheeseman, J. R., Scalmani, G., Barone, V., Petersson, G. A., Nakatsuji, H., Li, X., Caricato, M., Marenich, A. V., Bloino, J., Janesko, B. G., Gomperts, R., Mennucci, B., Hratchian, H. P., Ortiz, J. V., Izmaylov, A. F., Sonnenberg, J. L., Williams-Young, D., Ding, F., Lipparini, F., Egidi, F., Goings, J., Peng, B., Petrone, A., Henderson, T., Ranasinghe, D., Zakrzewski, V. G., Gao, J., Rega, N., Zheng, G., Liang, W., Hada, M., Ehara, M., Toyota, K., Fukuda, R., Hasegawa, J., Ishida, M., Nakajima, T., Honda, Y., Kitao, O., Nakai, H., Vreven, T., Throssell, K., Montgomery Jr. N., Staroverov, V. N., Keith, T. A., Kobayashi, R., Normand, J., Raghavachari, K., Rendell, A. P., Burant, J. C., Iyengar, S. S., Tomasi, J., Cossi, M., Millam, J. M., Klene, M., Adamo, C., Cammi, R., Ochterski, J. W., Martin, R. L., Morokuma, K., Farkas, O., Foresman, J. B., Fox, D. J. (2016). Gaussian 16, Revision B.01, Gaussian, Inc., Wallingford CT, GaussView 5.0. Wallingford, E.U.A.

[17] Wachters, A. J. H. (1970). Gaussian Basis Set for Molecular Wavefunctions Containing Third-Row Atoms. *The Journal of Chemical Physics*, *52*(3), 1033–1036. https://doi.org/10.1063/1.1673095

[18] Becke, A. D. (1993). Density-Functional Thermochemistry. III. The Role of Exact Exchange. *The Journal of Chemical Physics*, *98*(7), 5648–5656. https://doi.org/10 .1063/1.464913

[19] Lee, C., Yang, W., Parr, R. G. (1988). Development of the Colle-Salvetti correlation-energy formula into a functional of the electron density. *Physical review B 50th Anniversary Milestones*, *37*(2), 785. https://doi.org/10.1103/PhysRevB.37.785

[20] Barone, V., Cossi, M., Tomasi, J. (1998). Geometry optimization of molecular structures in solution by the

polarizable continuum model. *Journal of Computational Chemistry*, *19*(4), 404–417. https://doi.org/10.1002/(SICI)1096-987X(199803)19:4<404::AID-JCC3>3.0.CO;2-W

[21] Tomasi, J., Mennucci, B., Cammi, R. (2005). Quantum Mechanical Continuum Solvation Models. *Chemical Reviews*, *105*(8), 2999–3094. https://doi.org/10.1021/cr9904009

[22] Seredyuk, V. A., Vargalyuk, V. F. (2008). [Estimation of reliability of quantum-chemical calculations of electronic transitions in aqua complexes of transition metals]. Russian *Journal of Electrochemistry*, *44*(10), 1105–1112.

[23] Ye, Y., Sun, X., Zhang, Y, Han, X., Sun, X. (2022). A novel cell-based electrochemical biosensor based on MnO_2 catalysis for antioxidant activity evaluation of anthocyanins. *Biosensors and Bioelectronics*, 202, 113990. doi: 10.1016/j.bios.2022.113990

[24] Huang, Z. , Zou, J., Yu, J. (2020). Facile and Rapid Fabrication of Petal-like Hierarchical MnO_2 Anchored SWCNTs Composite and its Application in Amperometric Detection of Hydrogen Peroxide. *Journal of The Electrochemical Society,* 167, 067505. doi: 10.1149/1945-7111/ab7e1e

[25] Tian, Y., Deng, P., Wu, Y., Li, J., Liu, J., Li, G., He, Q. (2020). MnO_2 Nanowires-Decorated Reduced Graphene Oxide Modified Glassy Carbon Electrode for Sensitive Determination of Bisphenol A. *Journal of The Electrochemical Society,* 167, 046514. doi: 10.1149/1945-7111/ab79a7

[26] Li, S. , Lv, M.-M., Meng, J., Zhao, L. (2018). A 3D composite of gold nanoparticle-decorated MnO_2 -graphene-carbon nanotubes as a novel sensing platform for the determination of nitrite. *Ionics,* 24, 3177–3186. doi: 10.1007/s11581-017-2426-x

[27] Dawadi, S., Gupta, A., Khatri, M., Budhathoki, B., Lamichhane, G., Parajuli, N. (2020). Manganese dioxide nanoparticles: synthesis, applications and challenges. *Bulletin of Materials Science*, 43, 277. https://doi.org/10.1007/s12034-020-02247-8

[28] Siddiqui, S. I., Manzoor, O., Mohsin, M., Chaudhry, S. A. (2019). Nigella sativa seed based nanocomposite-MnO_2 /BC: An antibacterial material for photocatalytic degradation, and adsorptive removal of Methylene blue from water. *Environmental Research*, 171, 328–340. https://doi.org/10.1016/j.envres.2018.11.044

[29] Hastuti, E., Subhan, A., Amonpattaratkit, P., Zainuri, M., Suasmoro, S. (2021). The effects of Fe-doping on MnO_2: phase transitions, defect structures and its influence on electrical properties. *Royal Society of Chemistry Advances*, 11, 7808–7823. doi: 10.1039/D0RA10376D

[30] Julien, C. M., Mauger, A. (2017). Nanostructured MnO_2 as Electrode Materials for Energy Storage. *Nanomaterials*, *7*(11), 396. https://doi.org/10.3390/nano7110396

[31] Hashem, A. M., Abuzeid, H., Kaus, M., Indris, S., Ehrenberg, H., Mauger, A., Julien, C.M. (2018). Green synthesis of nanosized manganese dioxide as positive electrode for lithium-ion batteries using lemon juice and citrus peel. *Electrochimica Acta*, 262. doi : 10.1016/j.electacta.2018.01.024

[32] Shaeri, M. A., Bagheri Mohagheghi, M. M. (2022). Synthesis and Electrochemical Properties of Layered Birnessite MnO_2 /Activated Carbon Nanocomposite. *Journal of Electronic Materials, 51*(5), 1–21. doi:10.1007/s11664-022-09499-6

[33] El-Nemr, K. F., Balboul, M. R., Ali, M. A. (2014). Electrical and mechanical properties of manganese dioxide-magnetite-filled acrylonitrile butadiene rubber blends. *Journal of Thermoplastic Composite Materials, 29*(5), 704–716. https://doi.org/10.1177/0892705714533372

[34] Xia, H.-Y., Li, B.-Y., Zhao, Y., Han, Y.-H., Wang, S.-B., Chen, A.-Z., Kankala, R.K. (2022). Nanoarchitectured manganese dioxide (MnO_2)-based assemblies for biomedicine. *Coordination Chemistry Reviews*, 464 (2017). https://doi.org/10.1016/j.ccr.2022.214540

[35] Wu, M., Hou, P., Dong, L., Cai, L., Chen, Z., Zhao, M., Li, J. (2019). Manganese dioxide nanosheets: From preparation to biomedical applications. *International Journal of Nanomedicine,* 14, 4781–4800. doi: 10.2147/IJN.S207666

[36] Majidi, M. R., Farahani, F. S., Hosseini, M., Ahadzadeh, I. (2019). Low-cost nanowired α-MnO_2 /C as an ORR catalyst in air-cathode microbial fuel cell. *Bioelectrochemistry,* 125, 38–45. https://doi.org/10.1016/j.bioelechem.2018.09.004

[37] Siwawongkasem, K., Senanon, W., Maensiri, S. (2022). Hydrothermal Synthesis, Characterization, and Electrochemical Properties of MnO_2 -Titanate Nanotubes (MnO_2 -TNTs). *Journal of Electronic Materials*, 51, 3188–3204. doi:10.1007/s11664-022-09550-6

[38] Redkin, A. N., Mitina, A. A., Yakimov, E. E. (2022). Binder-Free MnO_2 /MWCNT/Al Electrodes for Supercapacitors. *Nanomaterials*, *12*(17), 2922. https://doi.org/10.3390/nano12172922

[39] Kalarikkandy, A. V., Sree, N., Ravichandran, S., Dheenadayalan, G. (2022). Copolymer-MnO_2 nanocomposites for the adsorptive removal of organic pollutants from water. *Environmental Science and Pollution Research*. https://doi.org/10.1007/s11356-022-22137-2